Available online at www.sciencedirect.com
SCIENCE DIRECT®
Journal of Sound and Vibration 266 (2003) 929–942
JOURNAL OF SOUND AND VIBRATION
www.elsevier.com/locate/jsvi

Multiple mode current flowing passive piezoelectric shunt controller

S. Behrens*, S.O.R. Moheimani, A.J. Fleming

School of Electrical Engineering and Computer Science, The University of Newcastle, University Drive, Callaghan NSW 2308, Australia

Received 16 January 2002; accepted 1 October 2002

Abstract

A method for multiple mode piezoelectric shunt damping will be presented in this paper. The proposed "current flowing" shunt controller has a number of benefits compared to previous shunt damping schemes; it is simpler to implement and requires small number of passive circuit elements. The passive control strategy is validated through experimentation on two piezoelectric laminated structures.

1. Introduction

Placing an electrical impedance across the terminals of a piezoelectric transducer, which is normally bonded to or embedded in the host structure, is referred to as piezoelectric shunt damping. As the piezo-laminated structure strains, an electrical charge forms on the terminals of the transducer. By placing an appropriate passive electrical impedance across the terminals of the transducer, the circuit network is capable of increasing the mechanical damping.

Forward [1], experimentally demonstrated the use of resistive and inductive–resistive resonant piezoelectric shunt circuits. Hagood and von Flotow [2] later presented an analytical model for resistive and inductive–resistive shunt dampened systems. Other researchers, such as Refs. [3–5], have attempted to extend shunt damping to multiple modes. Currently, single and/or multiple mode shunts require large inductors to dampen low-frequency modes. Consequently, active inductors are synthesized using operational amplifiers [6] and digital signal processor [7].

In this paper, we present a new passive multiple mode piezoelectric vibration dampener. The effect of the "current flowing" shunt controller is studied theoretically and then validated

*Corresponding author. Fax: +61-2-4921-6993.
E-mail address: sbehrens@ecemail.newcastle.edu.au (S. Behrens).

0022-460X/03/$ - see front matter
doi:10.1016/S0022-460X(02)01380-9

experimentally on two resonant structures. The current flowing shunt controller is similar in nature to "current blocking" circuits [5], as only a single piezoelectric transducer is used to control vibration of several modes. While achieving comparable performance to that of the current blocking shunt controller, the proposed controller has a number of advantages; it is simpler to implement as it requires a smaller number of components, requires no "floating" inductors [6], and the controller is inherently multiple mode and guaranteed to be stable.

The paper is organized as follows. Section 2 introduces a method for modelling a piezoelectric transducer. Section 3 considers two piezoelectric laminated structures. Subspace system identification is employed to obtain a model for each system. In Section 4, a method for modelling the piezoelectric composite system, i.e., the dampened structure is developed. Section 5, presents the proposed "current flowing" shunt controller. Section 6, reports experimental results that verify the proposed control scheme. Finally in Section 7, the paper is concluded.

2. Dynamic modelling for piezoelectric shunt damping

2.1. Piezoelectric model

Piezoelectric crystals have the unique ability to convert mechanical strain into electrical energy and vice versa. For vibration control, a thin layer of piezoelectric material, normally lead to titanate zirconate (PZT), is sandwiched between two conducting layers. This forms a piezoelectric transducer. The transducer is then glued to the surface of the flexible structure using a strong adhesive material.

A piezoelectric transducer behaves electrically like a capacitor C_p and mechanically like a stiff spring. It is common practice to model the piezoelectric element as a capacitor C_p in series with a strain-dependent voltage source v_p [2,8,9], as shown in Fig. 1. As discussed in Refs. [10,11], for small mechanical strains, the piezoelectric strain–voltage relations is relatively linear.

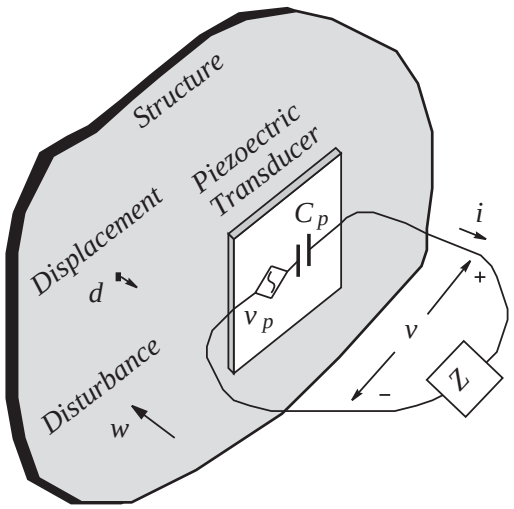

Fig. 1. A piezoelectric shunted structure.

2.2. Modelling the piezoelectric shunt system

Consider Fig. 1, where a piezoelectric transducer is adhered to the surface of a linear elastic structure. As the structure deforms, due to a point disturbance w, an electric charge forms on the conducting plates of the piezoelectric transducer. Since a charge has formed on the terminals of the piezoelectric transducer, a current flows through the impedance Z. Hence, mechanical energy is transformed to electrical energy which is subsequently dissipated by the resistive component of Z.

To make the discussion clearer, the shunt impedance Z is removed from the circuit, i.e., the piezoelectric transducer is open circuited, then the voltage across the terminals of the transducer is equivalent to v_p. The voltage v_p is entirely due to the disturbance w acting on the structure. Therefore, v_p is related to w via a transfer function G_{wv}. That is,

$$v_p(s) = G_{wv}(s)w(s), \quad Z(s) = \infty. \tag{1}$$

Alternatively, if we apply a voltage at v and measure the displacement at a point on the structure d, then the related transfer function between v to d is G_{vd}. Such that,

$$d(s) = G_{vd}(s)v(s), \quad Z(s) = \infty, \quad w(s) = 0. \tag{2}$$

Note the conditions $Z(s) = \infty$ and $w(s) = 0$, where the piezoelectric shunting layer terminals are open circuited and the point disturbance is set to zero, respectively.

Now, assume no disturbance is acting on the structure, i.e., $w(s) = 0$, while a voltage source $v(s)$ is attached to the terminals of the piezoelectric transducer. In this case, the transfer function from v_p to v is $G_{vv}(s)$. That is,

$$v_p(s) = G_{vv}(s)v(s), \quad w(s) = 0. \tag{3}$$

If the structure is disturbed by a voltage $\hat{v}$ applied to an identical collocated piezoelectric transducer and some impedance Z is attached to the piezoelectric terminals, then the overall linear relationship is

$$v_p(s) = G_{vv}(s)\hat{v}(s) - G_{vv}(s)v(s). \tag{4}$$

Furthermore, Ohm's law states that the voltage v is related to current i via

$$v(s) = Z(s)i(s). \tag{5}$$

Using Kirchoff's voltage law for Fig. 1, we can analyze the piezoelectric shunt circuit voltage v as

$$v(s) = v_p(s) - \frac{i}{C_p s}, \tag{6}$$

where C_p is the capacitance of the piezoelectric shunting layer. Using Eqs. (5) and (6), we obtain

$$v(s) = \frac{C_p s Z(s)}{1 + C_p s Z(s)} v_p(s). \tag{7}$$

Combining Eqs. (4) and (7) using simple algebra, we can find the shunt transfer function $\hat{G}_{vv}(s)$, as

$$\hat{G}_{vv}(s) = \frac{v_p(s)}{\hat{v}(s)} = \frac{G_{vv}(s)}{1 + G_{vv}(s)K(s)}, \tag{8}$$

where K is defined as

$$K(s) = \frac{C_p s Z(s)}{C_p s Z(s) + 1}. \tag{9}$$

Eq. (8) can also be used to obtain the displacement at a given point on the flexible structure, that is, the shunt transfer function $\hat{G}_{vd}(s)$, as

$$\hat{G}_{vd}(s) = \frac{d(s)}{\hat{v}(s)} = \frac{G_{vd}(s)}{1 + G_{vv}(s)K(s)}. \tag{10}$$

From the above equations, the reader may note that piezoelectric shunt damping is, in fact, a negative feedback control problem where K is the controller. For a more in-depth description of the shunt feedback scheme the reader is referred to Refs. [8,12].

3. Developing the "current flowing" shunt controller

The "current flowing" shunt is similar in nature to "current blocking" circuit [5]. Instead of preventing the current from flowing at a specific frequency ω_i $(i = 1, 2, 3, \ldots, n)$, we allow the current to flow. This is achieved by using a series capacitor–inductor circuit $C_i - \hat{L}_i$ as shown in Fig. 2. The series $C_i - \hat{L}_i$ is tuned to the structural resonance frequency ω_i. The series capacitor–inductor circuit, $C_i - \hat{L}_i$, appears to be a short circuit at ω_i and approximately open circuit for all other frequencies. While the shunting branch $\tilde{L}_i - C_p$ is also tuned to ω_i. Therefore, each circuit branch, $C_i - \hat{L}_i - \tilde{L}_i - R_i$, is functional at its own frequency ω_i, but is approximately open circuit at all other frequencies. Notice that some level of intereaction between modes that are closely spaced is expected. However, for modes that are widely spaced, this interaction will be minimal.

3.1. Example "current flowing" shunt controller for two modes

To illustrate the proposed shunt circuit, consider the two mode case shown in Fig. 3, at mode frequencies ω_1 and ω_2. The first branch of the shunt circuit, with shunt inductor $\tilde{L}_1 = 1/(\omega_1^2 C_p)$ and R_1, is inserted with a "current flowing" circuit consisting of a series capacitor and inductor circuit $C_1 - \hat{L}_1$ whose electrical impedance is designed to approach a short circuit at the branch

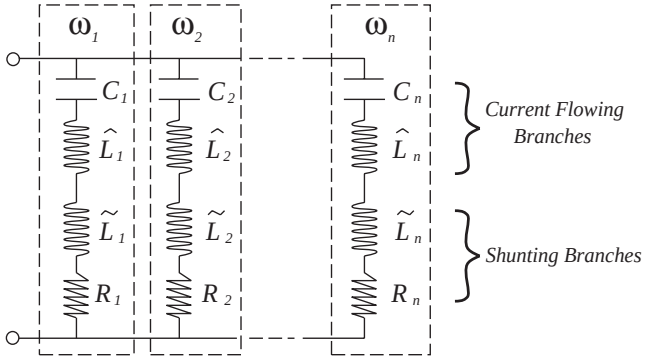

Fig. 2. Proposed "current flowing" multiple mode shunt circuit.

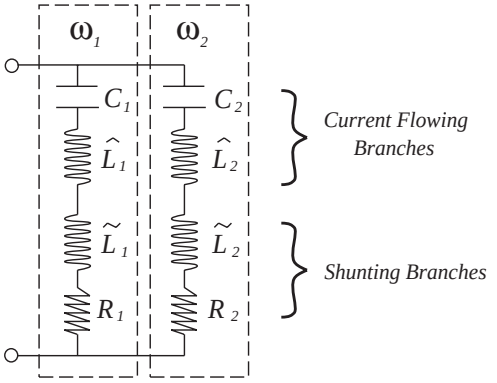

Fig. 3. Proposed two mode "current flowing" shunt circuit.

frequency of ω_1 (as indicated with ω_1 in Fig. 3). This is done by selecting C_1 and $\hat{L}_1$ such that the resonance frequency is at $\omega_1 = 1/\sqrt{C_1\hat{L}_1}$, which is a fundamental characteristic of any resonant capacitor–inductor circuit. The "current flowing" circuit in the second branch also uses a resonant circuit whose electrical impedance approaches a short circuit at the second structural frequency of ω_2 by selecting C_2 and $\hat{L}_2$ such that $\omega_2 = 1/\sqrt{C_2\hat{L}_2}$. When the two branches are connected together to the piezoelectric shunting layer terminals, each branch acts independently for their respective modes. That is, the first branch is designed to introduce damping at ω_1 while not disturbing the second branch that is approximately open circuit (i.e., the impedance is very large) at ω_1. The same reason applies for the second branch.

3.2. Generalized "current flowing" shunt controller

For the generalized case, for n structural modes,

$$\tilde{L}_1 = \frac{1}{\omega_1^2 C_p}, \ldots, \tilde{L}_n = \frac{1}{\omega_n^2 C_p}, \tag{11}$$

where $\tilde{L}_i$ is tuned into C_p. Frequencies ω_i are the mode frequencies to be passively controlled and assuming that $\omega_1 < \omega_2 < \cdots < \omega_n$. The relationship for $\hat{L}_i$ current flowing branches is

$$\hat{L}_1 = \frac{1}{\omega_1^2 C_1}, \ldots, \hat{L}_n = \frac{1}{\omega_n^2 C_n}. \tag{12}$$

By combining the series inductor values together (e.g., $L_i = \tilde{L}_i + \hat{L}_i$),

$$L_1 = \frac{C_p + C_1}{\omega_1^2 C_1 C_p}, \ldots, L_n = \tilde{L}_n + \hat{L}_n = \frac{C_p + C_n}{\omega_n^2 C_n C_p}, \tag{13}$$

the total impedance for each shunting branch $Z_i(s)$ has been simplified. Therefore, the *modified* current flowing shunt, shown in Fig. 4, has one less passive element in each shunting branch. The reader may note that the proposed *modified* controller, shown in Fig. 4, resembles the circuit of Hollkamp [4]. However, there are significant differences between the two approaches.

One distinction is that the shunt circuit proposed in Ref. [4] includes only one resistor–inductor circuit for the first mode, while in our approach a resistor–inductor–capacitor circuit is used to

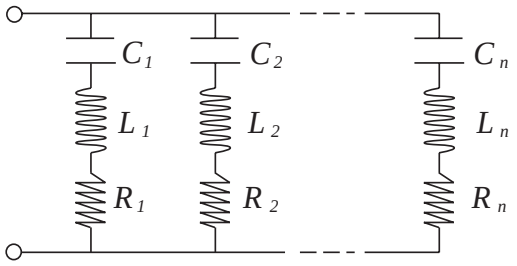

Fig. 4. Proposed modified "current flowing" multiple mode shunt circuit.

shunt each mode. Furthermore, the methodology proposed here for determining the capacitive and inductive elements is very different to that suggested in Ref. [4]. The reader can observe that by following the above procedure, capacitors and inductors for each parallel branch of the circuit can be determined in a very straightforward manner. This is in contrast to the methodology proposed in Ref. [4], that requires the solution to a non-trivial optimization problem.

The total shunt branch impedance $Z_i(s)$, is

$$Z_1(s) = \frac{s^2 + (R_1/L_1)s + 1/L_1C_1}{(1/L_1)s}, \ldots, Z_n(s) = \frac{s^2 + (R_n/L_n)s + (1/L_nC_n)}{1/L_ns}, \tag{14}$$

or the admittance $Y_i(s) = 1/Z_i(s)$ is

$$Y_1(s) = \frac{(1/L_1)s}{s^2 + (R_1/L_1)s + 1/L_1C_1}, \ldots, Y_n(s) = \frac{(1/L_n)s}{s^2 + (R_n/L_n)s + 1/L_nC_n}. \tag{15}$$

By summing the shunt branches together we derive the total shunt admittance as

$$Y(s) = \sum_{i=1}^{n} Y_i(s) = \sum_{i=1}^{n} \frac{(1/L_i)s}{s^2 + (R_i/L_i)s + 1/L_iC_i}. \tag{16}$$

Now, the feedback controller (9), can be determined as

$$K(s) = \frac{1}{1 + (1/C_ps)\,Y(s)}. \tag{17}$$

Using Eq. (16), it can be shown that the effective feedback controller is

$$K(s) = \frac{1}{1 + \sum_{i=1}^{n} \frac{1/(L_iC_p)}{s^2 + (R_i/L_i)s + 1/L_iC_i}} \tag{18}$$

or alternatively,

$$K(s) = \frac{\prod_{i=1}^{n}(s^2 + \frac{R_i}{L_i}s + \frac{1}{L_iC_i})}{\prod_{i=1}^{n}(s^2 + \frac{R_i}{L_i}s + \frac{1}{L_iC_i}) + \sum_{i=1}^{n} \frac{1}{L_iC_p} \prod_{l=1, l\neq i}^{n}(s^2 + \frac{R_l}{L_l}s + \frac{1}{L_lC_l})}. \tag{19}$$

Notice that the controller has a highly resonance structure. It applies a high gain at each target base structure resonant frequency. Viewing the shunted system in this manner has the advantage that the residual effects of each mode on other modes can be determined in a straightforward manner. It can be observed that as long as the controlled modes are reasonably spaced, this "residual effect" will be minimal. However, if two modes are very close, this effect cannot be

ignored and may degrade the performance of the shunted system at those specific resonance frequencies.

4. Proposed "current flowing" shunt controller validation

The validation proposed control scheme will be validated experimentally on two resonant structures; a simply supported beam, and a bounded plate structure. Photographs of the two piezoelectric laminate structures are shown in Figs. 5 and 6. For both structures, two piezoelectric patches are bonded to the surface of each structure using a strong adhesive material. On each structure, one piezoelectric patch will be used as an actuator to generate a disturbance and the other as a shunting layer, as shown in Fig. 7. For a detailed description of the apparatus, the reader is referred to Refs. [8,12,13].

In order to design an effective shunt controller it is necessary to obtain a model of the resonant system. Obtaining an analytic model for many realistic structure may not be possible since the flexible structure in question may be too difficult to model analytically. In such cases the technique of system identification may be helpful. Subspace-based system identification techniques have proven to be an efficient means of identifying the dynamics of high order, highly resonant systems. A full summary of subspace-based system identification techniques is described in Ref. [14].

When observing the dynamics of a structure, it is common practice to consider the transfer function between the displacement at some point on the structure and the disturbance actuator voltage applied to the actuating patch $G_{vd}(s)$. Another important transfer function is the dynamics between the shunting piezoelectric voltage (assuming $Z(s) = \infty$) and the actuator voltage. Since the shunting layer voltage and actuating voltage are collocated, as shown in Fig. 7, we can measure $G_{vv}(s)$ directly.

For the two resonant structures we need to experimentally minimize the energy of the system. This can be achieved by minimizing the $G_{vd}(s)$, i.e., the disturbance actuator voltage to the displacement at a point on the structure, as this effectively minimizes the vibration.

Using a Polytec laser scanning vibrometer (PSV-300) and a Hewlett-Packard spectrum analyzer (35670A), frequency responses were obtained for $G_{vd}(s)$ and $G_{vv}(s)$. These are shown plotted in Figs. 8 and 9, respectively. Using the subspace-based system identification technique, a model was

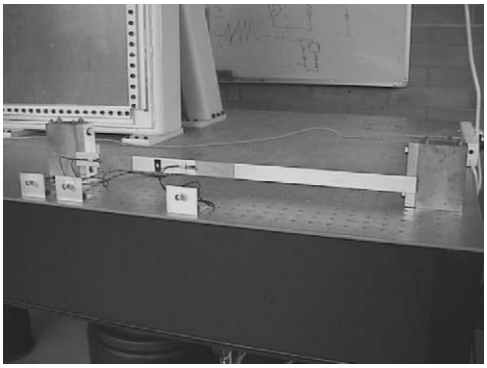

Fig. 5. Piezoelectric laminated simply supported beam.

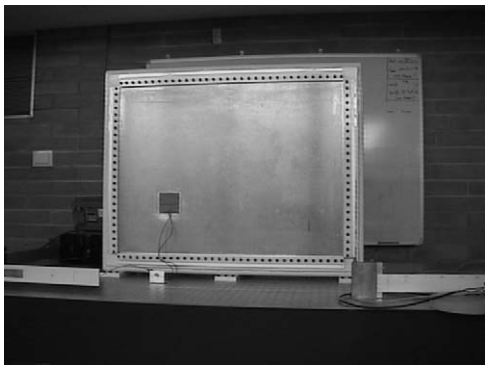

Fig. 6. Piezoelectric laminated plate bounded structure.

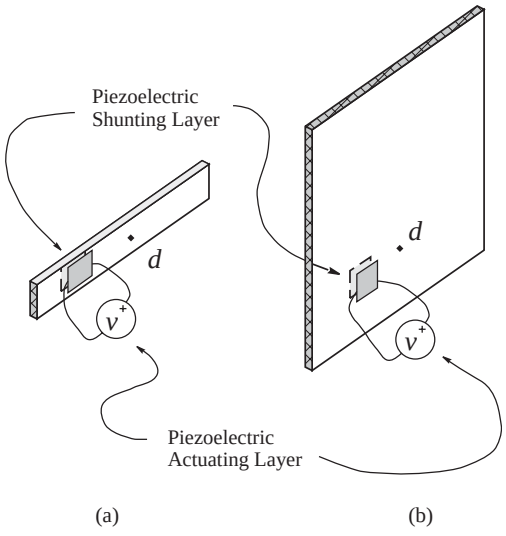

Fig. 7. Experimental piezoelectric laminated structures: (a) simply supported beam and (b) plate bounded structure. Note v is the applied disturbance actuator voltage and d is the displacement at some point on the structure.

fitted to the experimental data, the measured and identified transfer functions are shown in Figs. 8 and 9. In the bandwidth of interest, the identified models were found to be good representations of the piezoelectric laminated systems.

4.1. Simply supported beam

From Fig. 8, we can obtain the resonant modes of the laminated structure. The resonance frequencies for the structure are shown in Table 1. The second, third, fourth and fifth structural modes were chosen due to their highly resonant amplitudes.

Assuming the capacitance values C_2, C_3, C_4 and C_5 to be 10 nF and the experimentally measured piezoelectric shunt capacitance C_p is 105.77 nF, we can calculate the required inductance values using Eq. (13), as shown in Table 2.

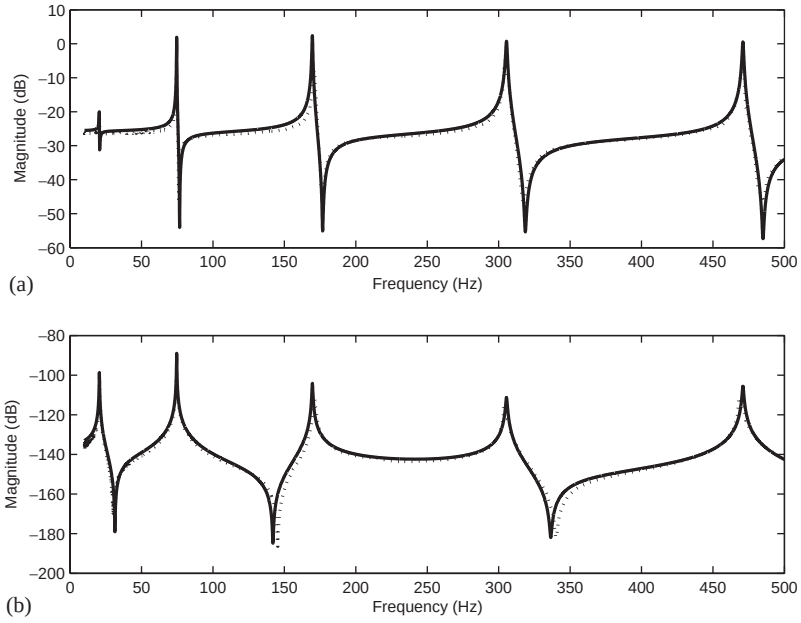

Fig. 8. Frequency response (a) $|G_{vv}(s)|$ and (b) $|G_{vd}(s)|$, for the piezoelectric laminated simply supported beam structure. Experimental data (···) and model obtained using subspace-based system identification (—).

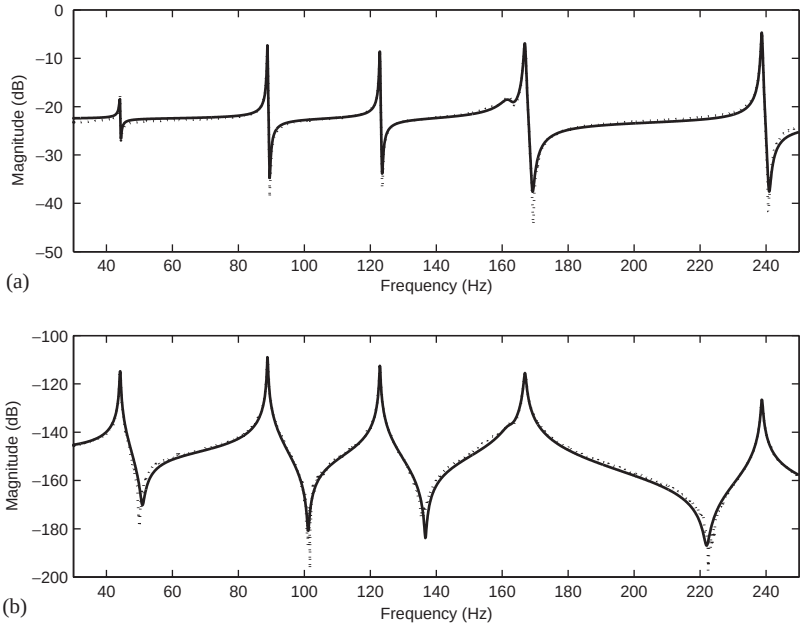

Fig. 9. Frequency response (a) $|G_{vv}(s)|$ and (b) $|G_{vd}(s)|$, for the piezoelectric laminated plate bounded structure. Experimental data (···) and model obtained using subspace-based system identification (—).

Table 1
Experimental resonant frequencies for the simply supported beam

Mode	Value (Hz)
ω_2	76
ω_3	173
ω_4	306
ω_5	472

Table 2
Circuit parameters for the simply supported beam

Circuit element	Value
L_2	480.0 H
L_3	92.6 H
L_4	29.6 H
L_5	12.4 H
R_2	1423 Ω
R_3	1212 Ω
R_4	913 Ω
R_5	798 Ω

In order to find the appropriate shunt resistance R_i, an optimization approach could be used. An optimization technique was proposed in Ref. [15], where the $\mathscr{H}_2$ norm of the controlled system is minimized. Optimal shunt resistance values obtained using this technique are displayed in Table 2.

Simulated results for $|G_{vd}(s)|$ and $|\hat{G}_{vd}(s)|$ the shunted transfer function from the disturbance voltage to displacement, show that the resonance amplitudes have been considerably dampened, as shown in Fig. 10. Table 3 summarizes the simulated amplitude reductions for the second, third, fourth and fifth modes.

Using a synthetic impedance[1] [7] with the required current flowing shunt circuitry, the frequency response of the shunted structure can be measured using the laser scanning vibrometer. Fig. 11 shows the experimentally measured displacement responses for $|G_{vd}(s)|$ and $|\hat{G}_{vd}(s)|$. The experimental resonant amplitudes were successfully reduced, as summarized in Table 3.

4.2. Plate bounded structure

Considering Fig. 9, we can obtain the resonance frequencies of the bounded structure, they are shown in Table 4. The first, second, third, fourth, fifth and sixth structural modes were chosen due to their high resonant amplitudes. The fourth mode was neglected due to the reduced control authority and its proximity to the fifth mode.

[1] The term "synthetic impedance" denotes a two terminal device that has an arbitrary relationship between voltage and current at its terminals, assuming that the admittance is stable and proper [7].

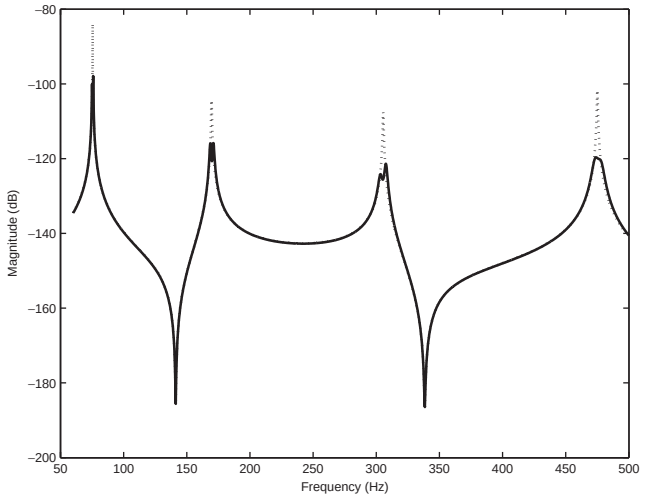

Fig. 10. Simulated beam frequency response: $|G_{vd}(s)|$ undamped response (⋯) and $|\hat{G}_{vd}(s)|$ damped response (—).

Table 3
Amplitude reduction for the simply supported beam

Mode	Simulated (dB)	Experimental (dB)
2	14.5	13.5
3	8.2	7.8
4	14.1	13.8
5	16.4	15.8

Setting C_1, C_2, C_3, C_5 and C_6 to be 7 nF, and C_p equal to 67.9 nF, we can calculate the required inductance values, as shown in Table 5. The already mentioned $\mathscr{H}_2$ norm optimization strategy is employed to determine the required resistance values, which are tabulated in Table 5.

Simulated results for $|G_{vd}(s)|$ and $|\hat{G}_{vd}(s)|$ show that the structural amplitudes of the resonant structure have been dampened, as shown in Fig. 12 and Table 6.

Using the synthetic impedance [7] and the laser scanning vibrometer, we can measure $|G_{vd}(s)|$ and $|\hat{G}_{vd}(s)|$. The frequency response for the experimental undamped and damped systems are shown in Fig. 13. Experimental results, shown in Fig. 13, demonstrate that the structural modes of the bounded structure have been considerably damped. The experimental resonant amplitudes were successfully reduced, as shown in Table 6.

5. Conclusion

The current flowing controller has been introduced as an alternative method for reducing structural vibrations. While achieving comparable performance to other passive control schemes, the current flowing piezoelectric shunt circuit has a number of advantages; it is simple—requires less resistors, capacitors and inductors; requires no "floating" inductors [6]; mode dominant—

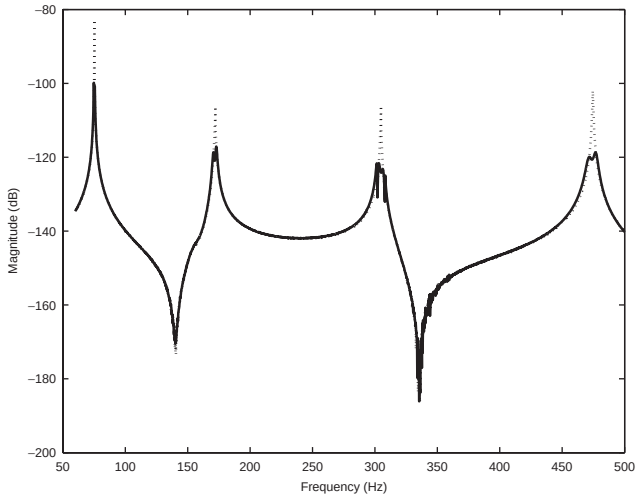

Fig. 11. Experimental beam frequency response: $|G_{vd}(s)|$ undamped response (⋯) and $|\hat{G}_{vd}(s)|$ damped response (—).

Table 4
Experimental resonant frequencies for the plate bounded structure

Mode	Value (Hz)
ω_1	44.85
ω_2	90.2
ω_3	124.2
ω_4	161.6
ω_5	167.6
ω_6	237.2

Table 5
Circuit parameters for the plate bounded structure

Circuit element	Value
L_1	1986.3 H
L_2	491.1 H
L_3	259.2 H
L_5	142.2 H
L_6	71.1 H
R_1	2498.2 Ω
R_2	1858.3 Ω
R_3	1272.6 Ω
R_5	1641.5 Ω
R_6	1400.1 Ω

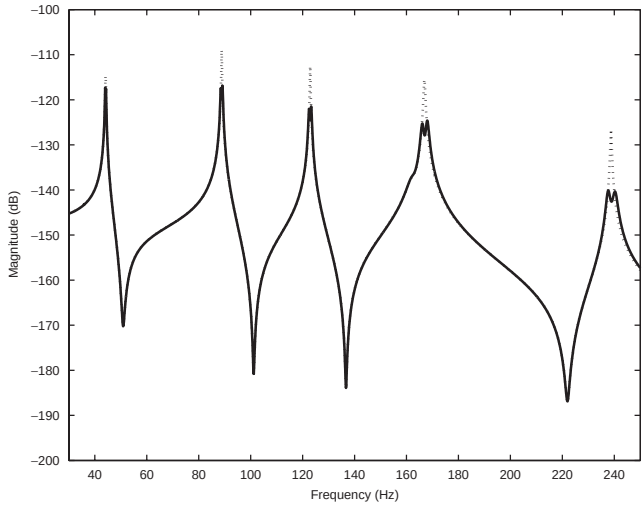

Fig. 12. Simulated plate frequency response: $|G_{vd}(s)|$ undamped response (⋯) and $|\hat{G}_{vd}(s)|$ damped response (—).

Table 6
Amplitude reduction for the plate bounded structure

Mode	Simulated (dB)	Experimental (dB)
1	3.2	3.8
2	10.9	10.1
3	13.2	12.8
5	13.9	13.2
6	15.8	14.7

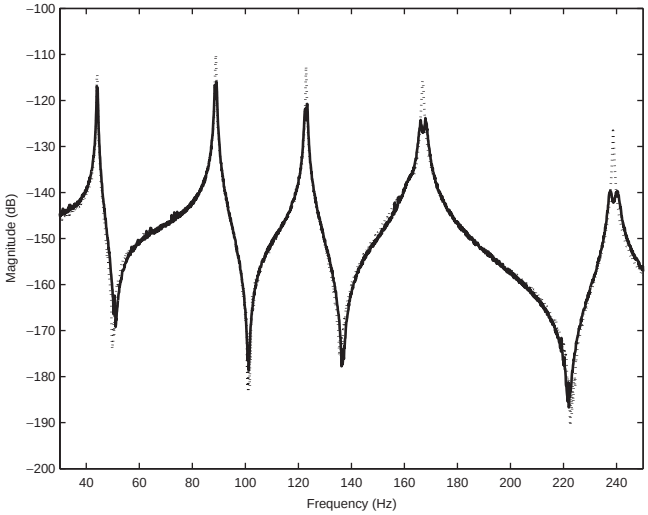

Fig. 13. Experimental plate frequency response: $|G_{vd}(s)|$ undamped response (⋯) and $|\hat{G}_{vd}(s)|$ damped response (—).

capable of damping more dominate resonant modes or neglecting the less dominant modes; multiple mode—can damp multiple modes using a single piezoelectric transducer; and passive—it is dissipative and guaranteed to be stable.

Acknowledgements

This research was supported by the Centre for Integrated Dynamics and Control (CIDAC) and the Australian Research Council (ARC).

References

[1] R.L. Forward, Electronic damping of vibrations in optical structures, Applied Optics 18 (1979) 690–697.
[2] N.W. Hagood, A.v. Flotow, Damping of structural vibrations with piezoelectric materials and passive electrical networks, Journal of Sound and Vibration 146 (2) (1991) 243–268.
[3] D.L. Edberg, A.S. Bicos, C.M. Fuller, J.J. Tracy, J.S. Fechter, Theoretical and experimental studies of a truss incorporating active members, Journal of Intelligent Materials Systems and Structures 3 (1992) 333–347.
[4] J.J. Hollkamp, Multimodal passive vibration suppression with piezoelectric materials and resonant shunts, Journal of Intelligent Materials Systems and Structures 5 (1994) 49–56.
[5] S.Y. Wu, Method for multiple mode shunt damping of structural vibration using a single PZT transducer, in: Proceedings of the SPIE Smart Structures and Materials, Smart Structures and Intelligent Systems, SPIE, Vol. 3327, 1998, pp. 159–168.
[6] R.H.S. Riodan, Simulated inductors using differential amplifiers, Electronics Letters 3 (2) (1967) 50–51.
[7] A.J. Fleming, S. Behrens, S.O.R. Moheimani, Synthetic impedance for implementation of piezoelectric shunt damping circuits, Electronics Letters 36 (18) (2000) 1525–1526.
[8] S. Behrens, Passive and semi-active vibration control of piezoelectric laminates, Master's Thesis, University of Newcastle, Australia, 2001.
[9] J.J. Dosch, D.J. Inman, E. Garcia, A self-sensing piezoelectric actuator for collocated control, Journal of Intelligent Material Systems and Structures 3 (1992) 166–185.
[10] C.R. Fuller, S.J. Elliott, P.A. Nelson, Active Control of Vibration, Academic Press, New York, 1996.
[11] B. Jaffe, W.R. Cook, H. Jaffe, Piezoelectric Ceramics, Academic Press, New York, 1971.
[12] S. Behrens, A.J. Fleming, S.O.R. Moheimani, New method for multiple-mode shunt damping of structural vibration using a single piezoelectric transducer, in: Proceedings in SPIE Smart Structures and Materials, Damping and Isolation, SPIE, Vol. 4331, 2001, pp. 239–250.
[13] D. Halim, S. Moheimani, An optimization approach to optimal placement of collocated piezoelectric actuators and sensors on a thin plate, Journal of Mechatronics, (2001), to appear.
[14] T. McKelvey, A.J. Fleming, S.O.R. Moheimani, Subspace based system identification for an acoustic enclosure, American Society of Mechanical Engineers Journal of Vibration and Acoustics 124 (3) (2002) 429–464.
[15] S. Behrens, S.O.R. Moheimani, Optimal resistive elements for multiple mode shunt-damping of a piezoelectric laminate beam, in: Proceedings in IEEE Conference on Decision and Control, 2001, pp. 4018–4023.